JOURNAL OF SOLID STATE CHEMISTRY 115, 420–426 (1995)

# Preparation and Crystal Structure Refinement of $Li_4Mn_5O_{12}$ by the Rietveld Method

Toshimi Takada,[1] Hiroshi Hayakawa, and Etsuo Akiba

*Department of Inorganic Materials, National Institute of Materials and Chemical Research, Higashi 1-1, Tsukuba, Ibaraki 305, Japan*

Received May 16, 1994; in revised form August 22, 1994; accepted August 29, 1994

**Well-crystallized $Li_4Mn_5O_{12}$ powder has been prepared by heating a eutectic mixture of lithium acetate LiOAc and manganese nitrate $Mn(NO_3)_2$ at 700°C for 1–3 days in an $O_2$ atmosphere. The Li and Mn content in the final products was determined from atomic absorption spectroscopy. The tetravalent manganese in the final product was found to be 95% based on the active oxygen content determined by $KMnO_4$ titration. The structure of $Li_4Mn_5O_{12}$ crystallites was refined by the Rietveld method from powder X-ray diffraction data as a cubic spinel, $a = 8.1616(5)$ Å, space group $Fd\bar{3}m$. $Li_4Mn_5O_{12}$ crystallites are stable at temperatures up to 600°C in oxygen but decompose to spinel $LiMn_2O_4$ and monoclinic $Li_2MnO_3$ at temperatures higher than 530°C in $N_2$.** © 1995 Academic Press, Inc.

## 1. INTRODUCTION

The typical cubic spinel $LiMn_2O_4$ (1) possesses a prototypic symmetry of $Fd\bar{3}m$, $(O_h^7)$, in which oxygen ions form a cubic-close-packed array occupying the 32*e* sites of the space group; Mn ions occupy the 16*d* sites (half of the octahedral sites) and Li ions occupy the 8*a* sites (one-eighth of the tetrahedral sites). The interstitial octahedral sites (16*c*), which are interconnected three-dimensionally by sharing common edges with six like near neighbors exactly as the 16*d* sites but shifted by half a lattice parameter in space, provide 3D conduction pathways for $Li^+$ ions. These structural characteristics make the spinel-type lithium manganese oxides practical as $Li^+$ adsorbents and cathode materials for electrochemical cells and rechargeable lithium batteries.

Extensive research has been directed toward the development and optimization of the lithium manganese oxide electrodes for rechargeable lithium batteries (2, 3). Thackeray and co-workers (4–6) have demonstrated that the $[Mn_2]O_4$ framework is capable of reversibly accommodating Li over a wide range (i.e., $Li_{0.4}[Mn_2]O_4$ to $Li_2[Mn_2]O_4$). Powder X-ray diffraction patterns of the extracted/inserted samples confirmed that the spinel framework remained intact during the extraction/insertion process. The lattice parameter, however, decreased from 8.24 Å for $LiMn_2O_4$ to 8.03 Å for λ-$MnO_2$ due to the extraction of $Li^+$ and the simultaneous dissolution of $Mn^{2+}$ resulting from the disproportionation reaction of $2Mn^{3+} \rightarrow Mn^{2+} + Mn^{4+}$. This leads to a decline in electrode capacity and consequently, poor rechargeability of lithium secondary batteries. Most approaches directed at reducing the portion of $Mn^{3+}$ have been limited to doping, whereby, another ion, such as Co, Ni, Fe, Mg, is used to replace $Mn^{3+}$. However, it has been revealed that doping is not very effective. Recently, Kock and co-workers (7–9) demonstrated that the $Mn^{4+}$ defective spinels $Li_2O \cdot yMnO_2$ ($y = 2$–4, or $Li_2Mn_4O_9$–$Li_4Mn_5O_{12}$) could be synthesized at temperatures below 400°C. Their preliminary results showed that $Mn^{4+}$ defective spinels possessed higher electrode capacity and better rechargeability than that of $LiMn_2O_4$.

Ooi and co-workers (10–12) have systematically investigated the $Li^+$ extraction/insertion reactions with spinel-type Li–Mn–O compounds for the development of $Li^+$ absorbents for the extraction of $Li^+$ ions from sea water. The acid-treated samples of $Li_{1-x}Mn_{2-z}O_4$ or λ-$MnO_2$ have shown excellent selectivity of $Li^+$ from sea water as compared to the existing absorbents. It has also been found that the oxidation state of manganese in the heat-treated precursor plays a very important role in the formation of $Li^+$ insertion sites. The spinel-type precursor with trivalent Mn such as $LiMn_2O_4$ gives a redox-type site on the basis of Eqs. [1] and [2], whereas the precursor with tetravalent Mn alone (such as $Li_4Mn_5O_{12}$) simply gives an ion-exchange-type site based on $Li^+/H^+$ ion exchange as shown in Eq. [3]:

$$4(Li)[Mn^{3+}Mn^{4+}]O_4 + 8H^+ \rightarrow 3(\diamond)[Mn^{4+}]_2O_4 + 4Li^+ + 2Mn^{2+} + 4H_2O \quad [1]$$

$$(\diamond)[Mn^{4+}]_2O_4 + nLiOH \rightarrow (Li_n\diamond_{1-n})[Mn_n^{3+}Mn_{2-n}^{4+}]O_4 + \frac{n}{2}H_2O + \frac{n}{4}O_2 \uparrow \quad [2]$$

[1] To whom correspondence should be addressed.



0022-4596/95 $6.00

$$(Li)[Li_{0.33}Mn^{4+}_{1.67}]O_4 + 1.33H^+ \rightarrow (H)[H_{0.33}Mn^{4+}_{1.67}]O_4 + 1.33Li^+. \quad [3]$$

The symbols ( ), [ ], and ◇ are, respectively, 8*a* tetrahedral sites, 16*d* octahedral sites, and vacant sites.The $Li^+$ extraction/insertion reaction occurs preferentially with ion-exchange-type sites. Consequently, the structural expansion/contraction or the disproportionation reaction $2Mn^{3+} \rightarrow Mn^{2+} + Mn^{4+}$ is suppressed. The high Li/Mn ratio of 0.8 for the $Mn^{4+}$ defective spinel $Li_4Mn_5O_{12}$ or $Li_{1.33}Mn_{1.67}O_4$ makes it particularly attractive for applications as a $Li^+$ selective absorbent.

The difficulty in synthesizing well-crystallized $Mn^{4+}$ defective spinels is due to the concomitant formation of $Mn^{3+}$ by the reduction of tetravalent manganese at 400°C and above. The reduction can be simply expressed in oxide forms by

$$2MnO_2 \rightarrow Mn_2O_3 + \frac{1}{2}O_2. \quad [4]$$

For a number of $Mn^{4+}$, $Li^+$-containing spinels of the type $LiMe^{a+}Mn^{4+}O_4$ (Me represents bivalent or trivalent metal ions) prepared at 750°C, Blasse (13) found that the content of active oxygen determined by titration was generally somewhat lower than theoretically expected, i.e., larger amounts of $Mn^{3+}$ were present in such compounds. He indicated that at temperatures below 400°C, it was, however, not possible to obtain single-phase reaction products owing to the low rate of solid state reaction. Recent studies conducted by Thackeray's group (8, 11) revealed that $Li_4Mn_5O_{12}$ crystallites obtained via the solid state reaction of $Li_2CO_3$ and $MnCO_3$ at 400°C, was an intermediate phase, or metastable. They indicated that $Li_4Mn_5O_{12}$ would decompose to the stable spinel $LiMn_2O_4$ and monoclinic $Li_2MnO_3$ (14, 15) at temperatures higher than 400°C.

This paper describes our synthesis and characterization of the well-crystallized $Li_4Mn_5O_{12}$. It will be shown that the oxidation state of manganese in the precursor plays an important role in the formation of the well-crystallized $Mn^{4+}$ defective spinels.Once $Li_4Mn_5O_{12}$ crystallites form, they are stable up to 600°C in oxygen. The results of structure refinements and quantitative phase analyses by the Rietveld method based on the powder X-ray diffraction data are presented.

## 2. EXPERIMENTAL

### 2.1. Preparation of Well-Crystallized $Li_4Mn_5O_{12}$

Preliminary synthesis was conducted using a variety of Li and Mn compounds as raw materials including lithium carbonate $Li_2CO_3$, nitrate $LiNO_3$, acetate LiOAc; manganese carbonate $MnCO_3$, nitrate $Mn(NO_3)_2$, and the oxides $Mn_2O_3$, $MnO_2$. It was found that lithium acetate dihydrate $LiOAc \cdot 2H_2O$, and manganese nitrate hexahydrate $Mn(NO_3)_2 \cdot 6H_2O$, were superior to other starting materials in the preparation of $Li_4Mn_5O_{12}$ for the following reasons:

(i) The extremely low melting points of $Mn(NO_3)_2 \cdot 6H_2O$ (28°C) and $LiOAc \cdot 2H_2O$ (70°C) make it possible to obtain a homogeneous liquid precursor. Also, it was found that a uniform eutectic was formed simply by heating them at 100°C.

(ii) The oxidation of $Mn(NO_3)_2$ and LiOAc occurred simultaneously at very low temperatures below 200°C, thereby converting the eutectic to a highly reactive solid phase $Mn^{4+}$ precursor consisting of manganese oxide $MnO_2$ and amorphous $Li_2O$.

The preparation process developed for $Li_4Mn_5O_{12}$ is schematically shown in Fig. 1. 99.9% pure $LiOAc \cdot 2H_2O$ and $Mn(NO_3)_2 \cdot 6H_2O$ were purchased from WAKO Pure Chemical Industries, Ltd. and used without further purification. First, 40.0 g of $Mn(NO_3)_2 \cdot 6H_2O$ and 11.373 g of $LiOAc \cdot 2H_2O$ (Li/Mn = 0.8 in mole) were placed in a 1000 ml separable flask and mixed at 100°C for 1 hr with stirring under flowing $O_2$ gas. The eutectic liquid thus obtained was slowly oxidized at 200°C for 6 hr in $O_2$. The solid obtained was then powdered and pelletized (5 mm thick, 10 mm in diameter). Finally, the pellets were heated in a silica tube to a temperature of 500–850°C at a rate of 100°C/hr with a cylinder electric furnace and held there for 1–2 days with 200 ml/min of $O_2$ flowing during the crystallization of $Li_4Mn_5O_{12}$. The samples thus obtained were labeled after the reaction temperature and duration as ANT500-2D, ANT600-2D, ANT700-2D, and ANT850-1D. Most characterizations were carried out on sample ANT700-3D which was prepared by heating at 500°C for 1 day and then at 700°C for 3 days to insure good crystallinity.

The standard spinel $LiMn_2O_4$ was prepared in air by the solid reaction of $Mn_2O_3$ and $Li_2CO_3$ in a 2 : 1 molar ratio. Initially, it was heated at 650°C for 12 hr in order to decompose the $Li_2CO_3$; this was followed by heating at 850°C for 24 hr. The monoclinic phase $Li_2MnO_3$ was prepared by the solid reaction in air of $Li_2CO_3$ and $MnCO_3$ in a 1 : 1 molar ratio at 800°C for 24 hr.

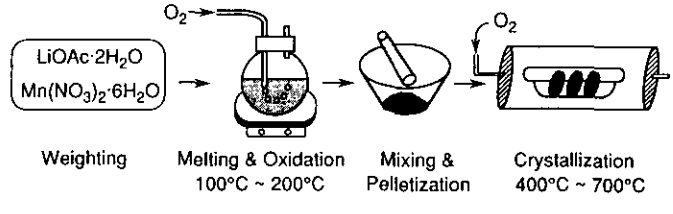


FIG. 1. Scheme for the preparation of well-crystallized $Li_4Mn_5O_{12}$.

### 2.2. Composition Analysis and Characterizations of $Li_4Mn_5O_{12}$

The Li/Mn molar ratio of the final products was determined using a Shimadzu AA-650 double beam digital atomic absorption spectrophotometer. The sample solution was prepared by first dissolving the sample in a solution of sulfuric acid and hydrogen peroxide, then evaporating the acids, and redissolving the solid in purified water. The standard solutions of Li (LiCl in 0.01 *N* HCl) and Mn ($Mn(NO_3)_2$ in 0.01 *N* $HNO_3$) at concentrations of 1000 ppm were purchased from WAKO Pure Chemical Industries Ltd., and used for calibration after diluting to 1–10 ppm with purified water. The mean oxidation number of manganese ($Z_{Mn}$) in the sample was determined from the active oxygen content as measured from the standard volumetric method (16) of $KMnO_4$ titration.

The density was evaluated from the buoyancy of the sample in toluene using ME-210250/21060 density determination kits and a METTLER AT261 analytical balance. A special gem holder with a Ta vessel (15 mm high, 10 mm in diameter) and a Cu wire holder (70 mm high, 0.2 mm in diameter), was especially designed for powder samples. In order to fully displace the air within the sample powder by toluene, the sample within the Ta vessel was immersed in 200 ml of toluene for 24 hr under low pressure (500 mmHg) before the measurement of buoyancy.

Powder X-ray diffraction patterns were collected at room temperature on a Rigaku RAX-I X-ray diffractometer with Cu$K\alpha$ radiation monochromated by a graphite single crystal at 40 kV, 30 mA. The structural refinement was carried out with the Rietveld refinement program *RIETAN* (17) on a Fujitsu M-1800/30 (MSP) mainframe computer.

The thermal stability of $Li_4Mn_5O_{12}$ was measured by TG using a Seiko SSC5020 thermal analyzer system at a heating/cooling rate of 10°C/min with 200 ml/min flow of $O_2$ or $N_2$.

## 3. RESULTS AND DISCUSSION

### 3.1. Characterization of Well Crystallized $Li_4Mn_5O_{12}$

Powder X-ray diffraction patterns of the products from reactions between LiOAc + $Mn(NO_3)_2$; $Li_2CO_3$ + $MnCO_3$; $Li_2CO_3$ + $MnO_2$; $Li_2CO_3$ + $Mn_2O_3$ at 700°C for 24 hr under flowing $O_2$ are shown in Fig. 2. By comparing the sharpness and heights of the main reflection peaks, it is clear that the main phase $Li_4Mn_5O_{12}$ synthesized from the eutectic of LiOAc + $Mn(NO_3)_2$ has the best crystallinity, whereas that from $Li_2CO_3$ + $MnCO_3$ has the worst. This can be attributed to the following facts: (i) The decomposition temperature of $MnCO_3$ (370°C) and $Li_2CO_3$ (>600°C) is much higher than that of $Mn(NO_3)_2$ (129.5°C)

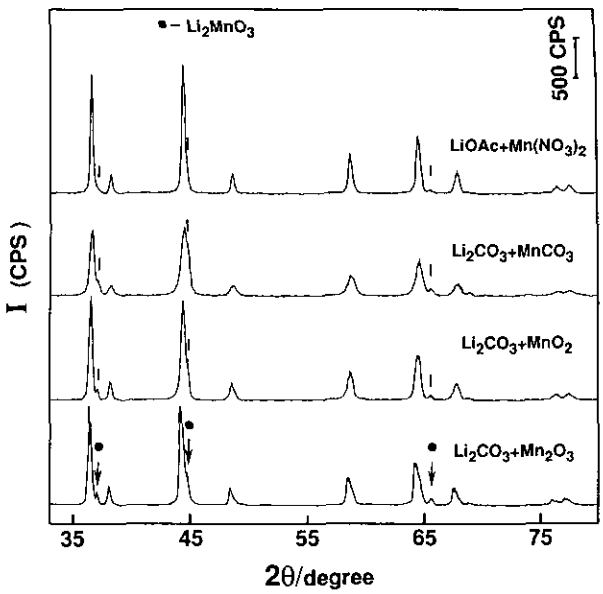


FIG. 2. Powder X-ray diffraction patterns of $Li_4Mn_5O_{12}$ samples prepared at 700°C from various raw materials.

and LiOAc (<200°), thereby retarding their ability to form $Li_4Mn_5O_{12}$. (ii) The precursor obtained from LiOAc + $Mn(NO_3)_2$ via liquid states should have higher uniformity and reactivity. Careful observation revealed that the magnitude of the shift of diffraction peaks to lower $2\theta$ values, as a result of the formation of $LiMn_2O_4$ and $Li_2MnO_3$, was in the order corresponding to the starting manganese compounds, $Mn_2O_3$ > $MnCO_3$ > $MnO_2$. Considering that $MnCO_3$ decomposes to a mixture of $MnO_2$ and $Mn_2O_3$ under the reaction conditions, it is evident that the trivalent $Mn^{3+}$ portion of the precursor has a strong tendency to form $LiMn_2O_4$, as well as $Li_2MnO_3$, which precipitates from the reaction, thereby consuming the surplus Li. Therefore, it is essential to use $Mn^{4+}$ precursors to synthesize well-crystallized $Li_4Mn_5O_{12}$.

The measured composition, active oxygen content, and density data of $Li_4Mn_5O_{12}$ prepared under various conditions are given in Table 1. The Li/Mn molar ratios in the samples prepared from the eutectic of LiOAc and $Mn(NO_3)_2$ (denoted as AN) were found to be exactly 0.8, indicating the high homogeneity of the precursor. However, the Li/Mn ratio of the sample prepared from $Li_2CO_3$ + $MnCO_3$ (denoted as CC) was 0.88 which is significantly higher than 0.8 and probably due to the inhomogeneity of the precursor and the localized precipitation of $Li_2MnO_3$. Overall, the active oxygen contents of $Li_4Mn_5O_{12}$ samples were calculated to be somewhat lower than that for the case where it is assumed that all manganese ions are tetravalent. The maximum percentage of $Mn^{4+}$ ($Mn^{4+}$%) in the samples was estimated from

TABLE 1
**Composition, Active Oxygen Content, and Density Data for $Li_4Mn_5O_{12}$ Samples Prepared under Various Conditions and, for Comparison, the Data for the Standards $LiMn_2O_4$ and $Li_2MnO_3$**

| Sample ID | Li/Mn (mole) | Density (g/cm³) | Active oxygen% | | Mn ion state | |
|---|---|---|---|---|---|---|
| | | | Calculated | Measured | $Z_{Mn}$ | $Mn^{4+}$% |
| ANT500-2D-$O_2$ | — | 3.91 ± 0.02 | 16.18 | 15.17 ± 0.04 | 3.75 | 93.7 |
| (10 atm) | | 3.91 ± 0.02 | | 15.15 ± 0.04 | 3.75 | 93.6 |
| ANT600-2D-$O_2$ | 0.80 ± 0.01 | 3.95 ± 0.02 | 16.18 | 15.12 ± 0.04 | 3.74 | 93.4 |
| ANT700-3D-$O_2$ | 0.80 ± 0.01 | 4.01 ± 0.02 | 16.18 | 15.36 ± 0.03 | 3.80 | 94.9 |
| (10 atm) | 0.80 ± 0.01 | 4.02 ± 0.02 | | 15.27 ± 0.03 | 3.78 | 94.3 |
| ANT850-2D-$O_2$ | — | 4.12 ± 0.03 | 16.18 | 15.10 ± 0.03 | 3.73 | 93.2 |
| CCT700-3D-$O_2$[a] | 0.88 ± 0.02 | 4.08 ± 0.03 | 16.18 | 14.79 ± 0.03 | 3.66 | 91.3 |
| $LiMn_2O_4$ | 0.50 ± 0.01 | 4.10 ± 0.03 | 13.27 | 13.36 ± 0.03 | 3.52 | 75.5 |
| $Li_2MnO_3$ | — | 3.87 ± 0.01 | 13.70 | 13.75 ± 0.03 | 4.01 | 100.3 |

[a] This sample was prepared by reacting $Li_2CO_3$ with $MnCO_3$ at 700°C for 3 days under flowing $O_2$.

the active oxygen content to be 95%. In an attempt to oxidize the $Mn^{3+}$ portion, the pressure of oxygen during the reaction and crystallization of the precursor obtained from LiOAc + $Mn(NO_3)_2$, was increased to 10 atm. The results for the sample synthesized under 10 atm of $O_2$ are shown in Table 1 along with those prepared under the same conditions but with flowing $O_2$. No improvement was observed in terms of the $Mn^{4+}$% in these samples. Hence, increasing the oxygen pressure to 10 atm was not sufficient to fully prevent the $Mn^{4+}$ from being reduced when the crystallization temperature was raised above 500°C. Based on these results, further characterization was limited to the samples prepared from LiOAc + $Mn(NO_3)_2$ with $O_2$ flowing.

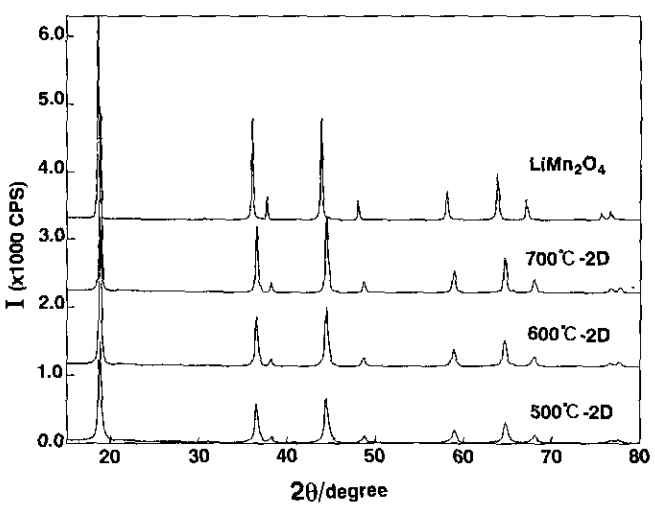


FIG. 3. Powder X-ray diffraction patterns of $Li_4Mn_5O_{12}$ samples prepared from the eutectic of LiOAc and $Mn(NO_3)_2$ at various temperatures, together with that of $LiMn_2O_4$. An offset of 1100 cps of each line was applied for clarity.

Figure 3 shows powder X-ray diffraction patterns of $Li_4Mn_5O_{12}$ prepared at 500, 600, and 700°C from LiOAc + $Mn(NO_3)_2$, and for comparison, the standard $LiMn_2O_4$ is also presented. Clearly, the higher reaction temperature gave the sharper and higher diffraction peaks, and consequently the better crystallinity of $Li_4Mn_5O_{12}$. The minor monoclinic phase $Li_2MnO_3$, however, became apparent as the reaction temperature was raised above 700°C. The diffraction peaks of monoclinic phase $Li_2MnO_3$ in the sample obtained at 700°C were negligible as shown in Figs. 2 and 3. All the detected reflection peaks were consistent with that of a cubic spinel $LiMn_2O_4$, but with a visible shift to the higher $2\theta°$ values corresponding to the contraction of the unit cell from $a = 8.242$ Å for $LiMn_2O_4$ to 8.1616(5) Å for $Li_4Mn_5O_{12}$.

Figure 4a shows the TG curve of sample ANT700-3D in $O_2$. The sample was fairly stable at temperatures up to 600°C. However, at temperatures between 700 and 400°C we observed what is, at least to our knowledge, the first example for such compounds of a reversible 0.77% weight loss/gain. By assuming that this weight loss/gain results from the desorption/absorption of oxygen due to the reduction/oxidation $Mn^{4+} \Leftrightarrow Mn^{3+}$

$$Li_4Mn_5^{4+}O_{12} \underset{\text{Cooling}}{\overset{\text{Heating}}{\rightleftharpoons}} Li_4Mn_x^{3+}Mn_{(5-x)}^{4+}O_{(12-\frac{x}{2})} + \frac{x}{4}O_2(g). \quad [5]$$

It is calculated that the 0.77% weight loss from 600 to 700°C leads to the evolution of 0.12 $O_2$ from one $Li_4Mn_5O_{12}$ with the reduction of 9.4% of $Mn^{4+}$ to $Mn^{3+}$, and upon cooling from 700 to 400°C, about 0.12 $O_2$ is absorbed from the atmosphere, i.e., $Li_4Mn_5^{4+}O_{12} \Leftrightarrow Li_4Mn_{0.48}^{3+}Mn_{4.52}^{4+}O_{11.76} + 0.12\ O_2$. Details about this reversible weight loss/gain will be described separately.

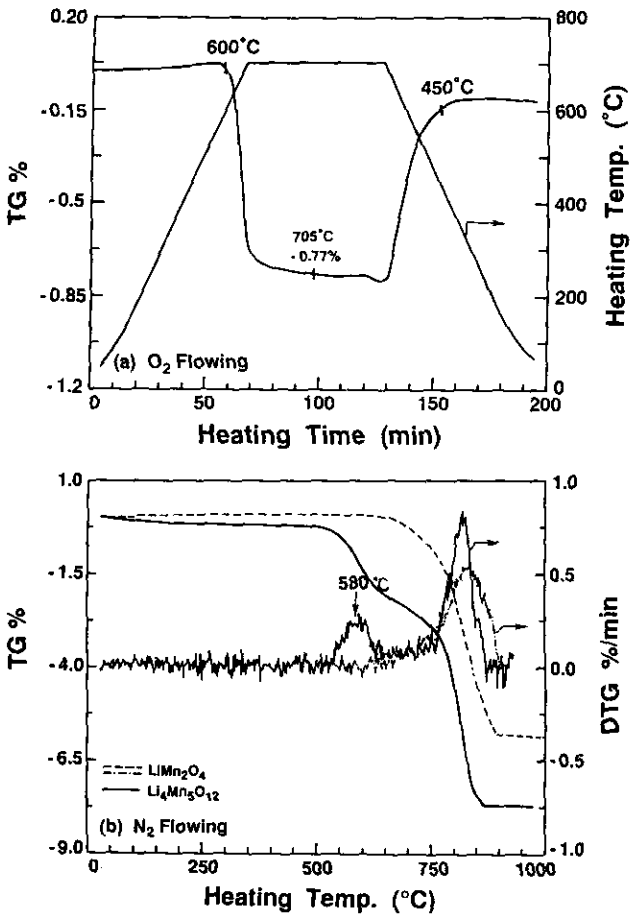


FIG. 4. TG-DTG curves of $Li_4Mn_5O_{12}$ (sample ANT700-3D) measured with the 200 ml/min flow of (a) $O_2$ and (b) $N_2$ together with that of $LiMn_2O_4$.

A significant effect of heating atmosphere on the stability of $Li_4Mn_5O_{12}$ was observed. Figure 4b shows the TG-DTG curves of sample ANT700-3D measured with flowing $N_2$, along with that of $LiMn_2O_4$ (the broken lines). The first weight loss (~3%) observed between 500 and 700°C can be attributed to the evolution of $O_2$ during the decomposition of $Li_4Mn_5O_{12}$ to $LiMn_2O_4$ and $Li_2MnO_3$ which corresponds to a weight loss of 3.24% according to

$$Li_4Mn_5O_{12} \rightarrow 2LiMn_2O_4 + Li_2MnO_3 + \frac{1}{2}O_2 \uparrow . \quad [6]$$

A second weight loss proceeds via the decomposition of $LiMn_2O_4$. The decomposition of $Li_4Mn_5O_{12}$ in $N_2$ was confirmed by X-ray diffraction data. Figure 5 shows the X-ray diffraction patterns of sample ANT700-3D after reheating at 580°C for 24 hr with 200 ml/min of $N_2$ or $O_2$ flowing. No structural change was detected in the sample reheated in $O_2$, but the structure of the sample reheated in $N_2$ changed remarkably as detected by the splitting and broadening of the reflection peaks. These peaks were assigned to the reflections from both $LiMn_2O_4$ and $Li_2MnO_3$. Consequently, the defective spinel $Li_4Mn_5O_{12}$ has better thermal stability in the oxygenic atmosphere than in a reductive atmosphere such as $N_2$.

### *3.2. Structure Refinement of $Li_4Mn_5O_{12}$ by the Rietveld Method*

Figure 6 shows the Rietveld refinement plot of sample ANT700-3D from which the structural data of $Li_4Mn_5O_{12}$ were determined; 5250 data points per scan were collected between $2\theta$ = 15°–120° with a step interval of 0.02°. The simultaneous refinement was carried out on two crystalline phases: phase 1-$Li_4Mn_5O_{12}$ (space group $Fd\bar{3}m$, No. 227) and phase 2-$Li_2MnO_3$ ($C/2m$, No. 12-1). The initial structure model for $Li_4Mn_5O_{12}/Li_{1.33}Mn_{1.67}O_4$ was adopted from Blasse's report (13). The crystallographic parameters of $Li_2MnO_3$ were adopted from Ref. (14) by Strobel and Lambert-Andron. Only the scale factor and cell parameters for $Li_2MnO_3$ were refined because of its small content (~5%). By performing a simultaneous refinement, the "goodness of fit" indicator, $S$, for $Li_4Mn_5O_{12}$ was improved from 1.46 for single phase refinement to 1.31. The improvements in $R$ factors for $Li_4Mn_5O_{12}$ ranged from: $R_{WP}$ = 16.06% to 14.48%, $R_P$ = 11.14% to 9.97%, $R_B$ = 2.72% to 2.02%, and $R_F$ = 2.27% to 1.74%, respectively. The crystallographic parameters of $Li_4Mn_5O_{12}$ are listed in Table 2. The site occupancy of the octahedrally coordinated manganese ions (16*d* sites) was refined as 0.84 with an estimated standard deviation (esd) of 0.02. This is in good agreement with 0.833 (1.67/2) of the ideal arrangement $Li_{1.33}Mn_{1.67}O_4$ (13) in which 0.33 Li ions are required to compensate for the imbalance in charge at the 16*d* sites. It is, however, very difficult to determine the occupancy of Li ions from X-

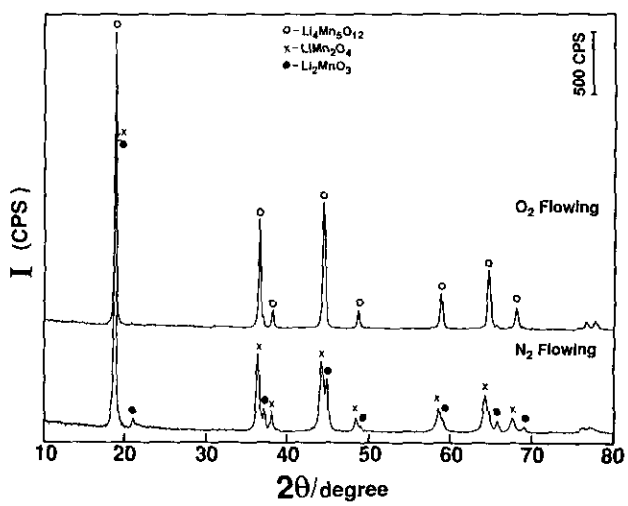


FIG. 5. Powder X-ray diffraction patterns of $Li_4Mn_5O_{12}$ (sample ANT700-3D) after reheating at 580°C for 24 hr with $O_2$ and $N_2$ flowing.

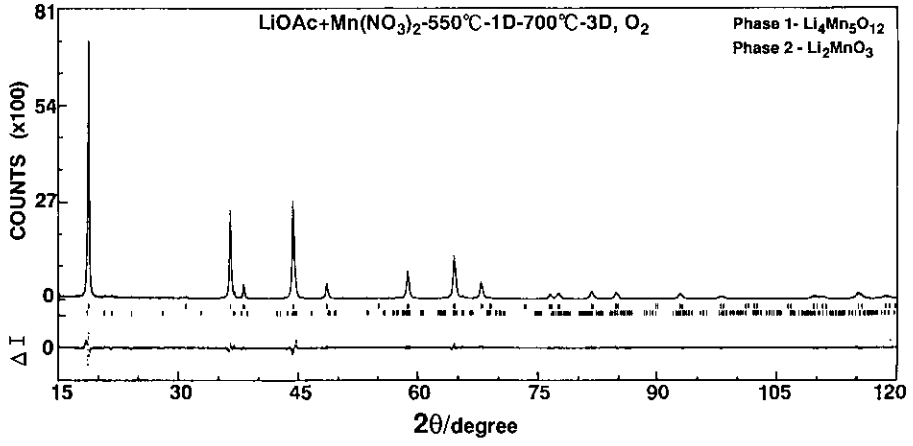


FIG. 6. Rietveld refinement plot of sample ANT700-3D. The observed and calculated intensity data ($I_o$ and $I_c$) are plotted in the upper field as points and as a solid-line curve, respectively. The difference $\Delta I = I_o - I_c$ is shown in the lower field. The tick marks below the pattern indicate the positions of all possible Bragg reflections from phase 1 (upper) and phase 2 (lower).

ray diffraction data, because Li is a light scatterer of X-rays and does not contribute much to the scattering amplitude of the individual reflections. For this reason, it is still not clear whether the presence of $Mn^{3+}$ will affect the distribution of Li ions on 16*d* sites. At this stage, we can conclude that the distribution of Li and Mn ions in $Li_4Mn_5O_{12}$ appears to be close to the ideal distribution $(Li)_{8a}[Li_{0.33}Mn_{1.67}]_{16d}O_4$. Further verification with neutron diffraction is in progress.

Efforts have been made to analyze the quantities of $Li_2MnO_3$ and $Li_4Mn_5O_{12}$ in the samples prepared at 500 850°C. Hill and co-workers (18–21) derived a very simple relationship for determining the phase abundance by the Rietveld method

$$W_p = S_p(ZMV)_p \Big/ \sum_{i=1}^{n} S_i(ZMV)_i,$$

where $W$ is the relative weight fraction of phase $p$ in a mixture of $n$ phase, and $S$, $Z$, $M$, and $V$ are, respectively, the Rietveld scale factor, the number of formula units per unit cell, the mass of the formula unit (in atomic mass units), and the unit cell volume. The amount of amorphous or noncrystalline material ($W_a$) in the sample was determined by adding Si powder in a weight fraction $W_s$, as an internal standard phase. In this case, the absolute weight fractions of the other identified components $p$ are given by

$$W_p = W_s S_p(ZMV)_p / S_s(ZMV)_s$$

and

$$W_a = 1 - \sum_{i=1}^{n} W_i.$$

The final results along with the lattice parameters and measured density data are shown in Table 3. Sample ANT700-3D had a high crystalline $Li_4Mn_5O_{12}$ content of 95%. Samples obtained at temperatures below 600°C contained about 2–6% of an amorphous component. Also an amount of crytalline $Li_2MnO_3$ and significant $LiMn_2O_4$ were observed in the sample prepared at 850°C. The amount of $LiMn_2O_4$ was determined from both Eq. [6] and the active oxygen content. The calculated densities of these samples, on the basis of the phase components

TABLE 2
**Crystallographic Parameters of $Li_4Mn_5O_{12}$ Crystal Prepared from LiOAc and $Mn(NO_3)_2$ at 700°C with Flowing $O_2$**

Space group: $Fd\bar{3}m$, No. 227, $a$ = 8.1616(5) Å, $S^a$ = 1.31

| Atom | Site | $x = y = z$ | $g$ | $B$ (Å$^2$) |
|---|---|---|---|---|
| Li(1) | 8*a* | 0.0 | 1.0 | 1.0 |
| Li(2)[b] | 16*d* | 0.625 | 0.16(2) | 0.72(6) |
| Mn | 16*d* | 0.625 | 0.84(2) | 0.72(6) |
| O | 32*e* | 0.3874(4) | 1.0 | 1.6(2) |

$R_{WP}$ = 14.48%, $R_P$ = 9.97%, $R_B$ = 2.02%, $R_F$ = 1.74%

*Note.* All numbers in parentheses represent the esd's. $g$ is the site occupancy.

[a] The "goodness of fit" indicator, $S$, and $R$ factors were defined as described on p. 22 of Ref. (17).

[b] Constraints on the site occupancy $g_{Mn} + g_{Li(2)} = 1$ and isotropic thermal parameter $B_{Mn} = B_{Li(2)}$ were applied.

TABLE 3
**Structural Parameters and the Results of a Quantitative Phase Analysis for $Li_4Mn_5O_{12}$ Samples by the Rietveld Method as well as for $LiMn_2O_4$ and $Li_2MnO_3$**

| Sample ID | $Li_4Mn_5O_{12}$ phase | | Calculated phase | | | Density (g/cm³) | |
|---|---|---|---|---|---|---|---|
| | $a$ (Å) | $g_{(Mn)}$[a] | ID | Density | % | Calculated | Measured |
| ANT500-2D | 8.1361(5) | 0.81(2) | $Li_4Mn_5O_{12}$ | 4.02 | 91.1 | — | 3.91(2) |
| | | | Amorphous | — | 6.0 | | |
| | | | $Li_2MnO_3$ | 3.91 | 2.9 | | |
| ANT600-2D | 8.1467(8) | 0.82(3) | $Li_4Mn_5O_{12}$ | 4.03 | 92.6 | — | 3.95(2) |
| | | | Amorphous | — | 2.0 | | |
| | | | $Li_2MnO_3$ | 3.90 | 5.4 | | |
| ANT700-3D | 8.1616(5) | 0.84(2) | $Li_4Mn_5O_{12}$ | 4.04 | 95.1 | 4.03 | 4.02(2) |
| | | | $Li_2MnO_3$ | 3.88 | 4.9 | | |
| ANT850-1D | 8.1813(5) | 0.85(9) | $Li_4Mn_5O_{12}$ | 4.07 | 80.6 | 4.10 | 4.12(3) |
| | | | $Li_2MnO_3$ | 3.88 | 6.5 | | |
| | | | $LiMn_2O_4$ | 4.39 | 12.9 | | |
| $LiMn_2O_4$ | 8.2411(4) | 0.95(7) | $LiMn_2O_4$ | 4.17 | 100 | 4.17 | 4.10(3) |
| $Li_2MnO_3$ | — | — | $Li_2MnO_3$ | 3.88 | 100 | 3.88 | 3.87(1) |

*Note.* Numbers in parentheses represent the error in the least significant figure.
[a] Site occupancy of the octahedrally coordinated manganese ions (16*d* sites).

determined by the Rietveld method, are close to the measured values within experimental error. Considering the difficulty in the synthesis of single phase $Li_4Mn_5O_{12}$, it is concluded that the quantitative phase analysis method provides indispensable information about the phase components.

## CONCLUSION

Well-crystallized $Li_4Mn_5O_{12}$ has been prepared from the eutectic of LiOAc and $Mn(NO_3)_2$ at 700°C for 1–3 days with $O_2$ flowing. The molar ratio of Li/Mn in the final products was determined to be exactly 0.80 from atomic absorption spectroscopy. The percentage of tetravalent manganese present in the final products was evaluated to be 95% based on active oxygen content. Rietveld refinement with powder X-ray diffraction data indicated that $Li_4Mn_5O_{12}$ possesses a cubic spinel structure with $a = 8.1616(5)$ Å, space group $Fd\bar{3}m$. $Li_4Mn_5O_{12}$ is stable in oxygenic atmosphere up to 600°C, but decomposes to $LiMn_2O_4$ and $Li_2MnO_3$ at 530°C in $N_2$.

## REFERENCES


1. D. G. Wickham and W. Groft, *J. Phys. Chem. Solids* **7,** 351 (1958).
2. M. M. Thackeray, *in* "Proceedings Mat. Res. Soc. Symposium Boston, Nov./Dec. 1988," Vol. 135, p. 585, 1989.
3. M. M. Thackeray, *in* "Proceedings, 5th International Seminar on Lithium Battery Technology and Application, Deerfield Beach, Florida, March 4–6, 1991."
4. M. M. Thackeray, W. I. F. David, P. G. Brouce, and J. B. Goodenough, *Mater. Res. Bull.* **18,** 461 (1983).
5. M. M. Thackeray, P. J. Johnson, L. A. Picciotto, P. G. Brouce, and J. B. Goodenough, *Mater. Res. Bull.* **19,** 179 (1984).
6. W. I. F. David, M. M. Thackeray, L. A. Picciotto, and J. B. Goodenough, *J. Solid State Chem.* **67,** 316 (1984).
7. A. de Kock, M. H. Rossouw, L. A. Picciotto, M. M. Thackeray, W. I. F. David, and R. M. Ibberson, *Mater. Res. Bull.* **25,** 657 (1990).
8. M. H. Rossouw, A. de Kock, L. A. Picciotto, M. M. Thackeray, W. I. F. David, and R. M. Ibberson, *Mater. Res. Bull.* **25,** 173 (1990).
9. M. M. Thackeray, A. de Kock, M. H. Rossouw, D. Liles, R. Bittihn, and D. Hoge, *in* "Proceedings, Electrochem. Soc.," Vol. 91-3, p. 326. 1991. [Proc. Primary Secondary Lithium Batteries, 1990]
10. K. Ooi, Y. Miya, and S. Katoh, *Solvent Extr. Ion Exch* **5**(3), 561 (1987).
11. K. Ooi, Y. Miya, and J. Sakakihara, *Langmuir* **7,** 1167 (1991).
12. Q. Feng, Y. Miya, H. Kanoh, and K. Ooi, *Langmuir* **8,** 1861 (1992).
13. G. Blasse, *Philips Res. Rep. Suppl.* **3,** 122 (1964).
14. P. Strobel and B. Lambert-Andron, *J. Solid State Chem.* **75,** 90 (1988).
15. A. Riou, A. Lecerf, Y. Gerault, and Y. Cudennec, *Mater. Res. Bull.* **27,** 267 (1992).
16. Japan Industrial Standard (JIS) M8233-1982, "Determination of Active Oxygen Content in Manganese Ores."
17. F. Izumi, *in* "The Rietveld Method" (R. A. Young, Ed.), p. 236. Oxford Univ. Press, New York, 1993.
18. R. J. Hill, *in* "The Rietveld Method" (R. A. Young, Ed.), p. 91. Oxford Univ. Press, New York, 1993.
19. R. J. Hill and C. J. Howard, *J. Appl. Crystallogr.* **20,** 467 (1987).
20. C. J. Howard, R. J. Hill, and M. A. M. Sufi, *Chem. Austral.* **Oct.,** 367 (1988).
21. R. J. Hill, *Powder Diffr.* **6**(2), 74 (1991).